Simulation of solute transport in a heterogeneous vadose zone describing the hydraulic properties using a multistep stochastic approach

Leonardo I. Oliveira,[1] Avery H. Demond,[1] Linda M. Abriola,[2] and Pierre Goovaerts[3]

Received 13 September 2005; revised 15 January 2006; accepted 31 January 2006; published 19 May 2006.

[1] The simulation of conservative solute transport in a heterogeneous unsaturated soil depends on the description of spatial variability of soil hydraulic and chemical properties. The data from the Las Cruces Trench Site were used to explore the impact of alternative ways of describing the variability of hydraulic properties. Three different approaches were considered: Miller and Miller scaling, Leverett scaling, and a multistep approach involving categorization of water retention curves. Conditional sequential geostatistical simulation was used to generate equally probable realizations of soil properties for each approach, and these realizations were then used as input to a numerical simulator to quantify the resultant uncertainty in solute transport predictions. Simulation results show that the scaling techniques seem to oversimplify the description of heterogeneity in the Las Cruces Trench, leading to very narrow spaces of uncertainty. Because the multistep approach allows the reproduction of existing patterns of continuity of soil classes and of contrasting values of hydraulic properties in the field, it led to solute plumes that split into several preferential pathways that were not observed in the simulations based on the scaling approaches, which increased the standard deviation of the solute plume's moments. The results indicate that measurements of both water retention curves and saturated hydraulic conductivity need to be collected for more realistic, conservative studies of flow in heterogeneous unsaturated soils.

Citation: Oliveira, L. I., A. H. Demond, L. M. Abriola, and P. Goovaerts (2006), Simulation of solute transport in a heterogeneous vadose zone describing the hydraulic properties using a multistep stochastic approach, *Water Resour. Res.*, *42*, W05420, doi:10.1029/2005WR004580.

1. Introduction

[2] The simulation of water flow and contaminant transport in a heterogeneous unsaturated soil requires a description of the spatial variability of the soil's unsaturated hydraulic conductivity and the soil water retention curves. Depending on the model assumed to represent these properties, one may need as many as six parameters, each one varying in space. To reduce the number of variables, focus is usually placed on those parameters which are deemed the most important: the soil water retention curve shape factors and the saturated hydraulic conductivity [*Jury et al.*, 1987b]. However, dealing even with this reduced number of parameters is not an easy task in a heterogeneous system: it usually requires a large number of measurements of the soil water retention curve and of the hydraulic conductivity which may be time consuming and costly to perform. Scaling theories, especially those of *Miller and Miller* [1956] and *Leverett* [1941], have been invoked to make up for the lack of data and have been widely used in both unsaturated [*Philip*, 1975; *Hopmans et al.*, 1988; *Russo*, 1991; *Tseng and Jury*, 1993; *Desbarats*, 1995; *Chen and Neuman*, 1996; *Rockhold et al.*, 1996; *Deurer et al.*, 2000; *Tartakovsky et al.*, 2003] and multiphase flow [*Essaid et al.*, 1993; *Dillard et al.*, 1997; *Gerhard and Kueper*, 2003] simulations. Using the Miller and Miller or the Leverett scaling theories, one can obtain a description of the variability of both hydraulic properties given data for only one of them. For example, the variability in saturated hydraulic conductivity can be used to estimate the variability in soil water retention [*Gerhard and Kueper*, 2003] and vice versa [*Rockhold et al.*, 1996].

[3] The appeal of the scaling approach is that it simplifies the description of the spatial variability of $\theta(\psi)$ and $K(\psi)$ to just one parameter, instead of two, three or even four, depending on the functions chosen to represent these relationships. The selection of such an approach implies, however, that, first, scaled water retention and scaled hydraulic conductivity curves will always have the same general shape and are shifted by a constant of proportionality, the scale factor, α. Yet, in a truly heterogeneous soil, it is very unlikely that these properties will have such similar shapes. The lack of proper reproduction of such patterns of variability in the description of soil properties could impact the predictions of water flow and the fate of contaminants in these systems. For example, *Lemke et al.* [2004], simulating DNAPL (dense nonaqueous phase liquid) entrapment and removal, observed notable differences in simulations using

[1]Department of Civil and Environmental Engineering, University of Michigan, Ann Arbor, Michigan, USA.
[2]Department of Civil and Environmental Engineering, Tufts University, Medford, Massachusetts, USA.
[3]BioMedware Inc., Ann Arbor, Michigan, USA.

0043-1397/06/2005WR004580

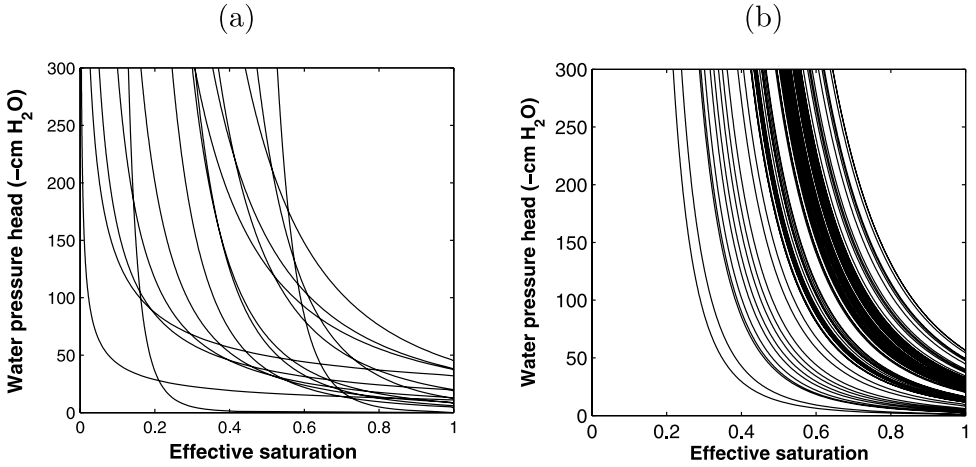

Figure 1. Example of (a) water retention curves measured in samples taken from the Las Cruces Trench Site and (b) scaled curves simulated using Miller and Miller scaling. The curves were fitted with the Brooks-Corey model.

models incorporating Leverett scaling of permeability and models utilizing uncorrelated air-entry pressure and permeability fields.

[4] Despite its widespread use, the scaling of hydraulic properties may be an oversimplification that potentially yields erroneous predictions of solute transport at the field scale. For example, Figure 1a shows a set of some typical soil water retention curves occurring in a natural field soil. The curves vary not only in shape but also frequently cross one another. Scaled curves, on the other hand, have the same general shape and never cross one another (Figure 1b). With this in mind, the objectives of this study are (1) to propose an alternative methodology for describing the soil hydraulic properties that more closely approximates the heterogeneous nature of real field soils and (2) to compare unsaturated zone transport simulation results obtained using the alternative method to those obtained using the scaling approaches.

2. Background

2.1. Unsaturated Flow and Transport Theory

[5] The equation describing the two-dimensional, isothermic, unsaturated transient flow of water in a nondeformable heterogeneous soil can be written as

$$\frac{\partial \theta}{\partial t} = \frac{\partial}{\partial x}\left[K_x(\psi)\frac{\partial \psi}{\partial x}\right] + \frac{\partial}{\partial z}\left[K_z(\psi)\left(\frac{\partial \psi}{\partial z} + 1\right)\right] - F \qquad (1)$$

where θ is the water content [L^3/L^3]; ψ is the water pressure head [L]; t is time [T]; x and z are the horizontal and upward vertical directions, respectively [L]; F is an external source or sink term (positive for sink) [T^{-1}]; $K_x(\psi)$ and $K_z(\psi)$ are the components of the unsaturated hydraulic conductivity tensor. In this study, the medium is assumed isotropic at the grid scale, and hysteresis is neglected.

[6] The movement of a single nonreactive solute in such a system is given by

$$\frac{\partial}{\partial t}(\theta C) = \frac{\partial}{\partial x}\left(\theta D_{xx}\frac{\partial C}{\partial x} + \theta D_{xz}\frac{\partial C}{\partial z}\right) - \frac{\partial}{\partial x}(v_x \theta C) + \frac{\partial}{\partial z}\left(\theta D_{zz}\frac{\partial C}{\partial z} + \theta D_{zx}\frac{\partial C}{\partial x}\right) - \frac{\partial}{\partial z}(v_z \theta C) - FC_s \qquad (2)$$

where C is the solute concentration [ML^{-3}]; C_s is the concentration of the source/sink term [ML^{-3}]; and D_{xx}, D_{zz}, $D_{xz} = D_{zx}$ are the components of the dispersion coefficient tensor [L^2T^{-1}], given by

$$D_{ij} = D_T|v|\delta_{ij} + (D_L - D_T)v_i v_j/|v| + \delta_{ij} D^* \tau_w \qquad (3)$$

where D^* is the coefficient of molecular diffusion [L^2T^{-1}]; τ_w is the tortuosity factor (dimensionless), given by $\tau_w = \theta^{7/3}/\theta_s^2$ [*Simunek et al.*, 1999]; D_L and D_T are the longitudinal and the transverse dispersivities [L] (here considered to be uniform throughout); δ_{ij} is the Kronecker delta function (i.e., $\delta_{ij} = 1$ if $i = j$, and $\delta_{ij} = 0$ if $i \neq j$); $|v| = \sqrt{v_x^2 + v_z^2}$; v_i and v_j are the ith and jth components of the pore water velocity [LT^{-1}], respectively, given by Darcy's law:

$$\vec{v} = -\frac{1}{\theta}K(\psi)\cdot\nabla(\psi + z) \qquad (4)$$

[7] To solve (1) numerically, one needs to parameterize the soil water retention and the unsaturated hydraulic conductivity curves. The Brooks-Corey relationship is assumed here to describe the soil water retention curve. It is given by [*Brooks and Corey*, 1964]

$$\Theta = \frac{\theta - \theta_r}{\theta_s - \theta_r} = \begin{cases} (|\psi_e|/|\psi|)^{\lambda} & \text{if } |\psi| > |\psi_e| \\ 1 & \text{otherwise} \end{cases} \qquad (5)$$

where Θ is the effective saturation (dimensionless); θ is the water content [L^3/L^3]; θ_s and θ_r are the saturated and residual water contents, respectively [L^3/L^3]; λ is the pore size index (dimensionless); and ψ_e is the air entry pressure head [L]. The unsaturated hydraulic conductivity is often estimated from the saturated hydraulic conductivity coupled with the soil water retention curve, using, for example, the Burdine model [*Burdine*, 1953] which, when coupled with the Brooks-Corey model, gives [*Brooks and Corey*, 1966]

$$K(\psi) = K_s\,\Theta^{3+2/\lambda} \qquad (6)$$

where K_s is the saturated hydraulic conductivity [LT^{-1}].

Table 1. Summary Statistics for $|\psi_e|$ Values Obtained With Multiple Linear Regression for Miller and Miller Scaling

	$\lvert\psi_e\rvert$, cm H_2O	ln $\lvert\psi_e\rvert$	α[a]
Minimum	0.088	−2.434	0.082
Mean	14.04	2.290	1.000
Median	11.73	2.462	0.403
Maximum	57.63	4.054	53.91
Standard deviation	10.23	0.979	3.034

[a]Here $\alpha = \psi_e^*/\psi_e$.

2.2. Stochastic Simulation of Soil Hydraulic Properties

[8] One way to deal with the uncertainty in soil hydraulic properties is to treat them as random space functions. As a consequence, the dependent variables (water pressure head, water content and solute concentration) are also random space functions [*Russo and Bouton*, 1992]. The generation of conditional spatially correlated random fields of soil properties may be easily accomplished within the geostatistical sequential simulation approach [*Deutsch and Journel*, 1998]. Each soil property is a regionalized variable, $z(\mathbf{u})$, that varies in space stochastically and represents a realization of a random function, $Z(\mathbf{u})$. Usually, $Z(\mathbf{u})$ is assumed to be second-order stationary, meaning that the expected value is invariant and the autocovariance does not depend on $\mathbf{u}$, only on the separation distance $\mathbf{h}$, such that

$$\mathrm{E}[Z(\mathbf{u})] = m \tag{7}$$

$$\mathrm{Cov}[Z(\mathbf{u}), Z(\mathbf{u}+\mathbf{h})] = C(\mathbf{h}) \tag{8}$$

Within this approach, equally probable realizations of a property, $z(\mathbf{u})$, are generated, each one reproducing: the measured values at sample locations; the sample histogram; and the covariance model [*Goovaerts*, 1997]. The approach to sequential simulation can be either parametric or nonparametric. In the parametric approach, a normal (Gaussian) function is chosen to describe the distribution of the property $z(\mathbf{u})$ or a transform of $z(\mathbf{u})$ (such as the logarithm of $z(\mathbf{u})$) so that its univariate distribution is completely characterized by the mean and the variance, and the bivariate distribution requires only the additional knowledge of the covariance function [*Deutsch and Journel*, 1998]. The process of sequential Gaussian simulation (SGS) involves a prior normal score transformation, in which the cumulative distribution function of the spatial attribute, $F(z)$, is converted into a standard cumulative distribution function, $G(y)$, with y having a standard probability density function with mean 0 and variance 1 [*Goovaerts*, 1997; *Deutsch and Journel*, 1998]. The simulations are made in the normal score space and then are back transformed using a one-to-one correspondence between $G(y)$ and $F(z)$.

[9] In the nonparametric (or indicator) approach, no assumption regarding the distribution of $z(\mathbf{u})$ has to be made. The cumulative distribution function (cdf) of $z(\mathbf{u})$ is divided into a number of classes which are used for a binary coding of each sample value based on whether, for continuous variables, $z(\mathbf{u})$ exceeds a class threshold [*Journel*, 1983] or, for categorical variables, it equals the probability of being no greater than a given class, which implies a ranking of these classes. In the latter case, the sequential indicator simulation (SIS) approach is used to generate realizations of categorical variables, which involves the prior coding of categorical attributes into indicator data as

$$i(\mathbf{u}; s_k) = \begin{cases} 1 & \text{if } s(\mathbf{u}) = s_k \\ & \qquad k = 1, \ldots, N_k \\ 0 & \text{otherwise} \end{cases} \tag{9}$$

where N_k is the number of categories.

[10] The indicator and the parametric sequential simulation techniques have been combined in what is known as the hierarchical or multistep approach [*Alabert et al.*, 1990; *Damsleth et al.*, 1992]. In this approach, the spatial variability of soil types (or facies) is modeled with indicator semivariograms for each class and then the spatial distribution of these classes is simulated. Therefore the distribution of major qualitative features, for instance, the distribution of coarse and fine soils, can be obtained. This step is then followed by the simulation of the properties of interest within each of these classes. In this way, the variability within each class is accounted for and distinct populations with distinct statistics can be dealt with, as shown by *Dillard et al.* [1997].

2.3. Scaling of Soil Hydraulic Properties

2.3.1. Miller and Miller Scaling

[11] According to the scaling approach for the description of the variability in soil water retention and unsaturated hydraulic conductivity, a single scaling factor, varying in

Table 2. Semivariogram Parameters[a]

Variable	γ_0	γ_1	a_{x1}, m	a_{z1}, m	γ_2	a_{x2}, m	a_{z2}, m	Str
ψ_e normal scores	0.17	0.70	6.28	2.09	0.11	50.0	1.83	Sph
K_s normal scores	0.12	0.75	4.79	1.87	0.13	12.14	1.87	Exp
Class 1 indicators	0.045	0.115	4.08	1.02	–	–	–	Sph
Class 2 indicators	0.107	0.016	1.63	0.40	–	–	–	Sph
Class 3 indicators	0.115	0.052	6.13	1.50	–	–	–	Sph
Class 4 indicators	0.102	0.028	2.09	0.52	–	–	–	Sph
Class 5 indicators	0.060	0.040	3.17	0.80	–	–	–	Sph
λ_1 normal scores	0.32	0.68	3.22	2.00	–	–	–	Sph
λ_2 normal scores	0.08	0.60	3.52	1.12	0.32	1000	2.0	Sph
λ_3 normal scores	0.61	0.39	2.55	1.17	–	–	–	Sph
λ_4 normal scores	0.13	0.52	4.34	2.15	0.45	1000	2.15	Sph
λ_5 normal scores	0.24	0.48	3.06	1.50	0.28	50	1.50	Sph

[a]The models are given by $\gamma(\mathbf{h}) = \gamma_0 + \gamma_1\,\mathrm{Str}\left(\frac{h_x}{a_{x1}} + \frac{h_z}{a_{z1}}\right) + \gamma_2\,\mathrm{Str}\left(\frac{h_x}{a_{x2}} + \frac{h_z}{a_{z2}}\right)$, where γ_0 is the nugget effect, γ_1 and γ_2 are contributions to the variance, a_{x1} and a_{x2} are the ranges in the horizontal direction h_x, and a_{z1} and a_{z2} are the ranges in the vertical direction h_z.

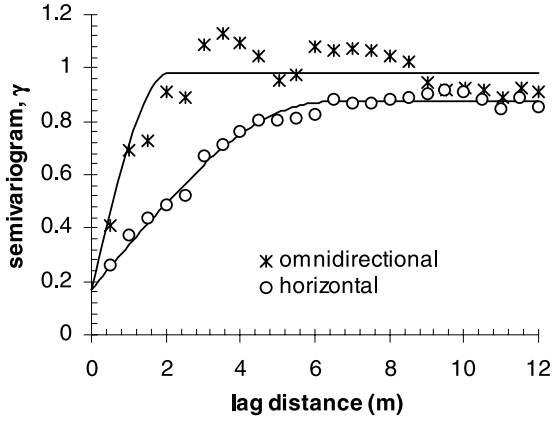

Figure 2. Experimental (symbols) and modeled (solid lines) normal score semivariograms for the air entry pressure head ψ_e.

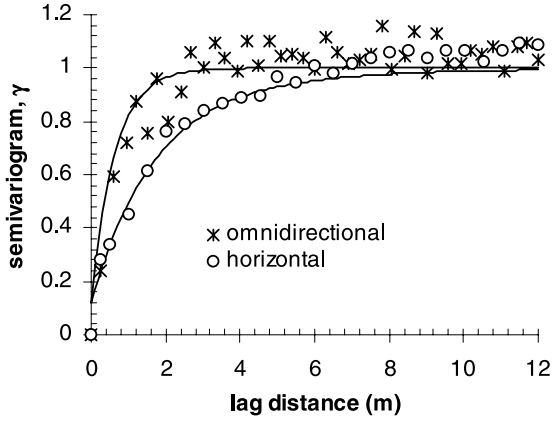

Figure 3. Experimental (symbols) and modeled (solid lines) normal score semivariograms for the saturated hydraulic conductivity, K_s.

space, is able to describe the ratio between each curve at a given point in space and their respective average curve over the entire range of water pressure heads [*Peck et al.*, 1977; *Ahuja et al.*, 1984; *Vogel et al.*, 1991; *Clausnitzer et al.*, 1992; *Hopmans*, 1992]. The scaling approach is derived from the similitude concept introduced by *Miller and Miller* [1955a, 1955b], which states that two porous media are similar if they have identical microscopic geometries and differ only in their scale. The water pressure head of a soil u, ψ_u, can be related to the water pressure head of a reference (or mean) soil, ψ^*, by a scaling factor, α_u, such that

$$\psi_u(\theta) = \frac{\psi^*(\theta)}{\alpha_u} \tag{10}$$

as long as both media are at the same water content, θ. Similarly, the two unsaturated hydraulic conductivities at the same θ, $K_u(\theta)$ and $K^*(\theta)$, are related by

$$K_u(\theta) = \alpha_u^2 K^*(\theta) \tag{11}$$

[12] The criterion for Miller and Miller similitude is rarely met in heterogeneous soils since soil structural properties vary spatially. Accordingly, *Warrick et al.* [1977] and *Russo and Bresler* [1980] relaxed some aspects of the Miller and Miller theory by, first, scaling by the degree of saturation ($S = \theta/\theta_s$) instead of by water content so that soils with different porosities could be scaled. Next, they assumed that the scale factor for the soil water retention curve would not necessarily have to be equal to the scale factor for the hydraulic conductivity curve. The result of relaxing these two assumptions is that dissimilar media can be scaled, although the scale factor loses its physical meaning, as it is no longer associated with a soil microscopic length. The scaling equations, then, become

$$\psi_u(S) = \frac{\psi^*(S)}{\alpha_{h_u}} \tag{12}$$

$$K_u(S) = \alpha_{K_u}^2 K^*(S) \tag{13}$$

where α_h and α_K are the scaling factors for the soil water retention and unsaturated hydraulic conductivity curves of a soil u, respectively. In the practical reality of contaminant transport studies, however, the unsaturated hydraulic curve is rarely measured and therefore is most often inferred from the parameters of the water retention curve, $\psi(S)$. Thus most scalings are performed only with respect to the water retention curve [*Shouse et al.*, 1995; *Rockhold et al.*, 1996; *Deurer et al.*, 2000]. When (5) is used to describe the soil water retention curve, all scaled water retention curves share the same pore size index, λ^*, and are shifted by a scaling factor that is the ratio between the air entry pressure head, ψ_e, and the air entry pressure head of the reference curve, ψ_e^*, such that

$$\alpha = \frac{\psi_e^*}{\psi_e} \tag{14}$$

Table 3. Summary Statistics for K_s Values Measured in Situ[a]

	K_s, m/d	log K_s	α
Minimum	0.093	−1.032	−1.032
Mean	8.780	0.614	1.000
Median	3.908	0.592	0.403
Maximum	129.98	2.114	53.91
Standard deviation	14.35	0.542	3.034

[a]Based on 489 values.

2.3.2. Leverett Scaling

[13] Another approach for scaling soil water retention curves was proposed by *Leverett* [1941], who found that experimental soil water retention curves from different unconsolidated sands could be plotted on the same curve, called the J function, when normalized in the following manner:

$$J(\Theta) = \frac{\psi}{\sigma}\sqrt{\frac{k}{n}} \tag{15}$$

where Θ is the effective saturation (dimensionless); σ is the surface tension [$ML^{-1}T^{-2}$], k is the intrinsic permeability of

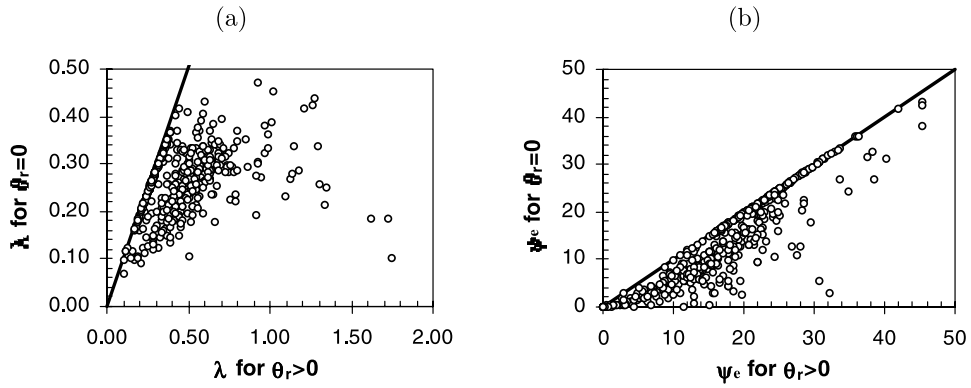

Figure 4. Comparison between values of (a) λ (dimensionless) and (b) ψ_e (cm H_2O) generated by fitting the Brooks-Corey model (equation (5)) with $\theta_r = 0$ and $\theta_r \geq 0$. The solid lines indicate a 1:1 match.

the porous medium [L^2], and n is its porosity (dimensionless). Through Leverett's scaling function (since intrinsic permeability (k) and saturated hydraulic conductivity (K) are directly related [*Bear*, 1972]), two different media containing the same fluid can be related to one another by

$$\psi_u(\Theta) = \sqrt{\frac{K^*}{K_u}\frac{n_u}{n^*}}\,\psi^*(\Theta) \tag{16}$$

where the superscript * refers to the reference soil and the subscript u refers to a different soil. If porosity is considered uniform, then Leverett scaling yields

$$\psi_u(\Theta) = \frac{\psi^*(\Theta)}{\alpha_u}\ ;\ \alpha_u = \sqrt{K_u/K^*} \tag{17}$$

which then gives

$$K_u = \alpha_u^2\, K^* \tag{18}$$

Equations (17) and (12) are similar to one another, only differing on the definition of their scaling factors. When only the saturated hydraulic conductivity is considered, equations (18) and (13) are also similar. Usually, the terms "Miller scaling" or "similar media" are used when the soil water retention curves are the primary information for describing the spatial variability in soils [*Desbarats*, 1995] and "Leverett scaling" is used when the saturated hydraulic conductivity is the primary source [*Gerhard and Kueper*, 2003], although sometimes they are used interchangeably [*Essaid et al.*, 1993; *Dillard et al.*, 1997], perhaps because of the convergence of the two theories.

[14] Studies of the impact of variability in soil water retention curves have already been published but they usually resort to the use of hypothetical data fields that are generated based on a prior knowledge of the spatial correlations of the soil hydraulic parameters [*Russo*, 1991; *Harter and Yeh*, 1996, 1998; *Russo et al.*, 1998, 2001; *Zhang and Lu*, 2002]. For example, *Harter and Yeh* [1996] investigated the influence of local measurements of saturated hydraulic conductivities and soil water tension using conditional simulation for predicting solute transport in five hypothetical soils. On the other hand, *Essaid et al.* [1993], *Rockhold et al.* [1996], and *Dillard et al.* [1997] used data on soil hydraulic properties (either measured or inferred) collected at real sites to generate only single simulation of the properties' spatial variability, precluding an assessment of the uncertainty arising from the description of the soil heterogeneity. In this study, only data on soil hydraulic properties collected at a real field site were used to compare the impact of different ways of describing their spatial variability on solute transport simulations, with no a priori assumptions made regarding the characteristics of the soil hydraulic properties at the site. Also, the uncertainty in solute transport predictions associated with each approach was investigated through the simulation of multiple realizations.

3. Methods

3.1. Field Site Database

[15] The soil hydraulic properties used in this study are those in the Las Cruces Trench Site database [*Wierenga*

Table 4. Summary Statistics for the Brooks-Corey Parameters Assuming Either $\theta_r \geq 0$ or $\theta_r = 0$[a]

	Assuming $\theta_r \geq 0$				Assuming $\theta_r = 0$			
	θ_s	θ_r	$\lvert\psi_e\rvert$, cm H_2O	λ	θ_s	θ_r	$\lvert\psi_e\rvert$, cm H_2O	λ
Minimum	0.218	0	1.20×10^{-5}	0.101	0.218	0	2.22×10^{-7}	0.070
Mean	0.322	0.051	17.18	0.467	0.322	0	13.51	0.259
Median	0.320	0.064	17.19	0.420	0.320	0	12.30	0.263
Maximum	0.529	0.133	45.45	1.743	0.529	0	42.99	0.471
Standard deviation	0.033	0.038	8.545	0.242	0.033	–	9.26	0.067

[a]Based on 448 values.

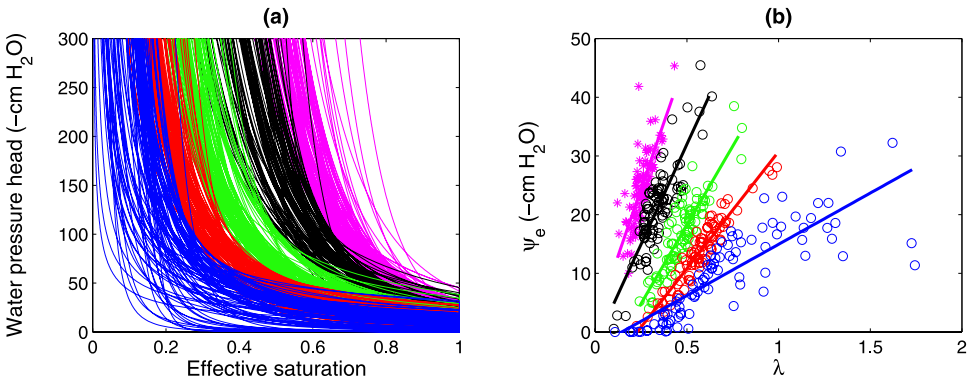

Figure 5. (a) Soil water retention classification using quantiles of Θ_{100} as dividers and (b) scatterplots of λ and ψ_e values (class 1, blue; class 2, red; class 3, green; class 4, black; class 5, magenta).

et al., 1989]. The database was generated as part of a comprehensive field study near Las Cruces, New Mexico, undertaken for testing deterministic and stochastic flow and transport models in the unsaturated zone [*Wierenga et al.*, 1991]. A 24.6 m long by 6.0 m deep trench wall was excavated and 450 samples were taken at nine layers, with 50 equally spaced samples per layer. The saturated hydraulic conductivity was measured in undisturbed samples in the laboratory and 489 measurements were made in situ with a borehole permeameter, 30 cm offset from where the samples were collected. Soil water retention curves were determined for 448 samples with the water content measured at water pressure heads of −10, −20, −40, −80, −120, −200, −300 cm H_2O as well as at −1, −5 and −15 bar. More information on the data collection methodology and the experimental protocols is given by *Wierenga et al.* [1989]. The soil characterization and infiltration experiments at this site have been analyzed in a number of articles [*Wierenga et al.*, 1991; *Jacobson*, 1990; *Hills et al.*, 1991; *Rockhold et al.*, 1996] and reports [*Wierenga et al.*, 1990; *Hills and Wierenga*, 1991; *Hills et al.*, 1993].

3.2. Simulation of Soil Properties

[16] All geostatistical simulations of soil properties were conditioned, within each approach, using the entire data set available (448 sets of water retention curves or 489 measurements of saturated hydraulic conductivity). The geostatistical domain was 25 m wide and 6 m deep, with a 10 cm spacing grid, entailing the simulation of 15,000 grid cells. The high sampling density of the data mitigated the destructuration effect (lack of correlation of extreme values) commonly associated with SGS. Since the spacing of the geostatistical grid is approximately the size of the sample support, there was no need for upscaling the soil properties. Experimental semivariograms were calculated and zonal, anisotropic models were fitted using a combination of nested structures of either spherical models (Sph), given by

$$\gamma(h) = \begin{cases} c\left[1.5\left(\frac{h}{a}\right) - 0.5\left(\frac{h}{a}\right)^3\right] & \text{if } h \le a \\ c & \text{if } h > a \end{cases} \quad (19)$$

or exponential models (Exp) given by

$$\gamma(h) = c\left[1 - \exp\left(-\frac{3h}{a}\right)\right] \quad (20)$$

where c is the variance contribution, h is the distance separating two locations, and a is either the actual (in (19)) or the effective (in (20)) range of the models. The sequential Gaussian simulations and the sequential indicator simulations were performed by the GSLIB programs SGSIM and SISIM, respectively [*Deutsch and Journel*, 1998].

3.2.1. Miller and Miller Scaling

[17] To implement the Miller and Miller scaling, the multiple linear regression method with "dummy" variables described by *Draper* [1981] was implemented and applied to the 448 sets of capillary pressure head–water content points in the Las Cruces data set. This technique, suggested by *Rockhold et al.* [1996], requires that θ_r be equal to 0. Only the data for pressure heads between −40 cm $H_2O \le \psi \le$ −300 cm H_2O were considered here, following the guidelines of *Corey and Brooks* [1999]. A single slope $\lambda^* = 0.2631$ was obtained as a result of the regression analysis with values for $|\psi_e|$ ranging from 0.087 cm H_2O to 57.63 cm H_2O. The values and the summary statistics obtained here (Table 1) are in very good agreement with those presented by *Rockhold et al.* [1996].

[18] In addition to the slope and intercept, one needs a value of air entry pressure for the reference curve, ψ_e^*, and a reference saturated hydraulic conductivity, K_s^*, to complete the soil characterization. Since most scaling techniques require that the mean of the scaling factors be equal to 1 [*Warrick et al.*, 1977; *Russo and Bresler*, 1980;

Table 5. Results of Regression Analysis of $|\psi_e|$ Versus λ (Equation (22))

Class	a	b	σ	R^2	F^a
1	17.47	−2.53	4.20	0.69	193.5
2	39.89	−9.14	1.91	0.89	702.1
3	53.66	−8.58	2.97	0.78	313.5
4	68.04	−2.05	3.80	0.73	238.0
5	90.75	1.68	4.00	0.63	151.24

[a]Values of $F \ge 6.73$ indicate that the hypothesis that the regression slope is equal to zero can be rejected with a 99% confidence.

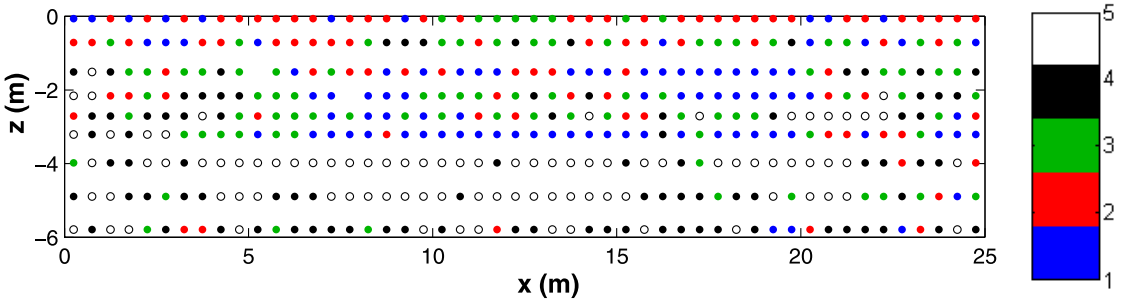

Figure 6. Spatial distribution of soil water retention curve classes in the Las Cruces Trench.

Clausnitzer et al., 1992], the reference value for ψ_e^* was taken as the ψ_e value that, when used in (14), provided a set of 448 scaling factors with a mean of 1. For this data set, ψ_e^* was found to be -4.728 cm H_2O. Given the direct relationship between ψ_e and α, and also the need to use a normal score transform in the SGS approach, simulating either ψ_e or α would result in the same spatial variability structure. Therefore the values of ψ_e were directly transformed to normal scores and a directional, zonal anisotropic semivariogram was modeled. The semivariogram parameters are listed in Table 2. The vertical component was approximated as the omnidirectional semivariogram since the data configuration did not allow the estimation of a strictly vertical semivariogram. The horizontal component, on the other hand, showed a very well defined structure, as shown in Figure 2.

[19] The geometric mean of the measured saturated hydraulic conductivity values is typically used as a reference value for scaling [*Rockhold et al.*, 1996; *Dillard et al.*, 1997]. Accordingly, the value of 4.11 m/d was used for K^*. One hundred realizations of the spatial distribution of ψ_e were generated and the saturated hydraulic conductivity field was obtained from (14) and (18):

$$K = \alpha^2 K^* = \left(\frac{\psi_e^*}{\psi_e}\right)^2 K^* \tag{21}$$

3.2.2. Leverett Scaling

[20] The 489 in situ measurements of saturated hydraulic conductivity were used to determine the scaling factors for the Leverett scaling approach. The values of K_s follow a lognormal distribution; the statistics are summarized in Table 3. As in the Miller and Miller approach for ψ_e, the K_s^* value that provided a set of 489 scaling factors with a mean of 1 was found to be 6.043 m/d. Since the scaling factors are a direct rescaling of K_s values, they also follow a lognormal distribution.

[21] The K_s values were transformed to normal scores and the omnidirectional, as well as the directional, horizontal semivariograms were calculated (the data configuration did not allow the estimation of vertical semivariograms). The spatial variability of the normal scores of K_s was modeled using a combination of anisotropic, exponential models (Table 2) where the vertical semivariogram was assumed to be identical to the omnidirectional semivariogram (Figure 3). One hundred realizations of K_s field were generated, from which soil water retention curves were derived through the application of (17). The reference values for λ^* and ψ_e^* were taken as 0.2631 and -4.728 cm H_2O, respectively, as determined in the Miller and Miller scaling.

3.2.3. MultiStep Approach

[22] To preserve the information about the soil water retention curves seen in Figure 1a, an approach based on a multistep or hierarchical stochastic simulation of soil properties [*Alabert et al.*, 1990; *Damsleth et al.*, 1992; *Dillard et al.*, 1997] may be useful. In this approach, the spatial distribution of soil classes (or facies) is simulated first, followed by the simulation of the properties of interest within these classes. To implement such an approach here, the same 448 sets of water content–pressure head data used in the Miller and Miller scaling were fit with (5), following the guidelines of *Corey and Brooks* [1999]. θ_r was taken as the value that provided the best fit of (5) to the logarithm of the values of Θ and $|\psi|$. Using nonzero values for θ_r resulted in significantly different values for λ from those obtained assuming $\theta_r = 0$, as shown in the scatterplots in Figure 4. The best fit θ_r values ranged from 0 to 0.13. Zero was the best fit value for θ_r for only 141 out of 448 samples, leading to significant differences in the statistics of ψ_e and λ (Table 4).

[23] Since the water content at $\psi = -100$ cm H_2O seems to capture the breadth of variation in the soil water retention curve, the effective saturation at a water pressure head of -100 cm H_2O, Θ_{100}, was determined for the 448 fitted water retention curves. The population of soil water retention curves was then divided into 5 classes of equal size using as limits the 20th, 40th, 60th, and 80th percentiles of the cumulative density function of Θ_{100}, namely, 0.278, 0.376, 0.512, and 0.657 (Figure 5a). Following this classification, five clusters of ψ_e versus λ values appear on the scatterplot (Figure 5b). Each cluster can be modeled by

$$|\psi_{e_i}| = a_i\lambda + b_i + \epsilon_i; \quad i = 1 \ldots 5 \tag{22}$$

where a_i and b_i are the slopes and intercepts of the line describing class i, and ϵ_i is the random deviation of the

Table 6. Summary Statistics of λ Values Within Each Soil Class

Class	Minimum	Mean	Median	Maximum	Standard Deviation
Class 1	0.108	0.698	0.629	1.743	0.355
Class 2	0.226	0.572	0.570	0.991	0.135
Class 3	0.242	0.472	0.479	0.800	0.104
Class 4	0.101	0.339	0.331	0.603	0.092
Class 5	0.121	0.255	0.251	0.432	0.057

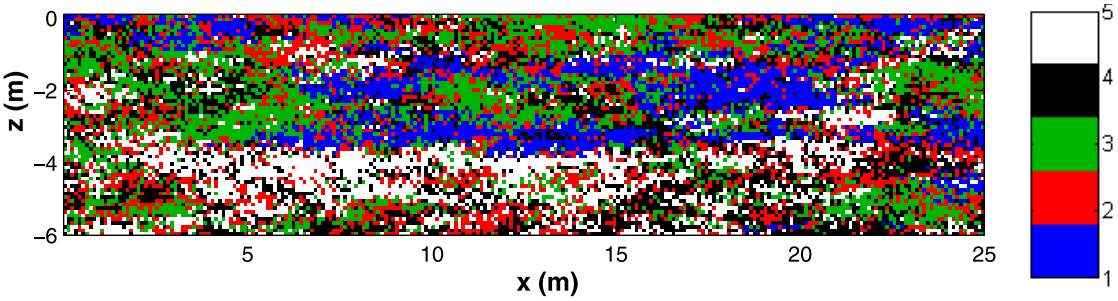

Figure 7. Example of a realization of the simulated distribution of classes.

model for each class, assumed to follow a normal distribution with mean 0 and variance $\sigma^2{}_i$, $\epsilon_i \in N(0, \sigma_i^2)$ [*Draper*, 1981]. The values of a_i, b_i, and σ_i are shown in Table 5, along with the coefficient of determination, R^2, and the statistic from the F test of significance of the regression, F. The R^2 values reveal that moderate to good regression is achieved. A higher proportion of variance could be explained with the addition of more classes; however, sufficient data must be present in each class to allow a good modeling of the spatial variability and the conditioning of the realizations to hard data. The use of Θ_{100} as a classification criterion is not unique. A similar breakdown into classes to that shown in Figure 5a was obtained evaluating $d|\psi|/d\Theta$ at $\Theta = 0.9$; however, there was more overlap between classes using this method than using the quantiles of Θ_{100} [*Oliveira*, 2004].

[24] To generate different realizations of soil properties, first, the spatial distribution of the five classes of soil water retention curves was simulated using sequential indicator simulation (SIS). Figure 6 shows the spatial distribution of soil classes in the Las Cruces Trench profile. Class 5 (the most difficult to drain) dominates the bottom of the soil profile whereas class 1 (the easiest to drain) prevails in the upper middle section. The remaining classes are scattered throughout the profile. Class indicator semivariograms were calculated and modeled [*Oliveira*, 2004] as anisotropic with the vertical range taken as approximately one fourth of the observed horizontal range. The parameters of the semivariogram models are listed in Table 2.

[25] Next, the values of λ were analyzed and simulated for each class separately. This is necessary because, as the statistics listed in Table 6 show, the expected values and standard deviation of λ differ from one class to another. Using this approach assures that the statistics and the spatial structure of λ within each class are reproduced, and that the values of ψ_e fall within the expected range. The values of λ were transformed to normal scores, for which semivariograms were calculated and then modeled with the parameters shown in Table 2 (semivariogram graphs can be found in *Oliveira* [2004]). Finally, statistics of the residual water content, θ_r, were different among classes. The average values of θ_r in classes 4 and 5 were 0.030 and 0.015, respectively, which are considerably different from the average value of 0.080 found for θ_r in classes 1, 2 and 3. Therefore these values were used in the multistep approach, in an attempt to generate soil realizations as close to reality as possible. The average saturated water content, θ_s, ranged from 0.318 to 0.327; therefore the value of 0.32 was used for all classes, the same value used with the scaling approaches. In those, θ_r was set equal to 0.05, the average value found in the original data set.

[26] To incorporate the uncertainty about the spatial distribution of soil classes and λ values, the two-stage approach suggested by *Damsleth et al.* [1992] was implemented here. Ten realizations of the distribution of soil classes were generated, each one coupled with ten realizations of λ values, resulting in one hundred realizations of soil water retention curves. The ψ_e value assigned to each grid cell was determined by the value of λ and the appropriate form of (22) for the soil class assigned to the same grid cell. Given the randomness introduced by the last term in (22), positive or very small values of $|\psi_e|$ could be predicted, in which case ϵ_i was set to 0 to assure a realistic soil representation. Such corrections were made, on average, to 1.5% of the grid cells. ψ_e values that were not reproduced at sampling locations could have been corrected a posteriori, but it was deemed unnecessary here since the number of simulated values is much larger than the number of sampled data. Figure 7 shows one realization of the spatial distribution of soil classes. Figure 7 shows that the predominance and continuity of classes 1 and 5 at their respective regions of occurrence are reproduced very well by the model (these two classes have lower relative nugget effect values). Class 3 is distributed in a patchy pattern

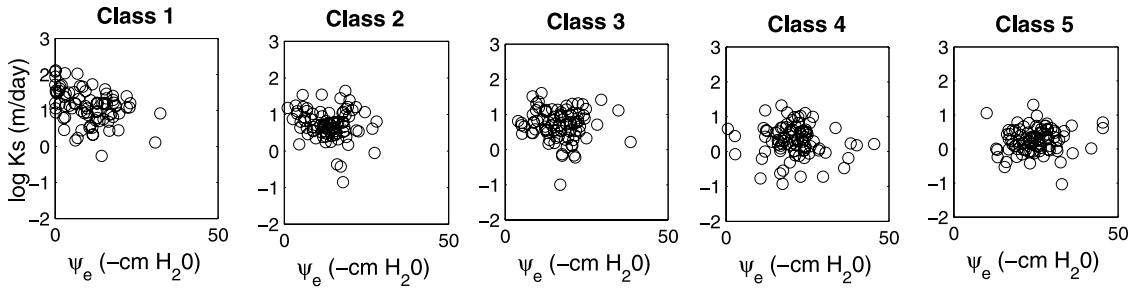

Figure 8. Scatterplot of log K_s versus ψ_e within each class.

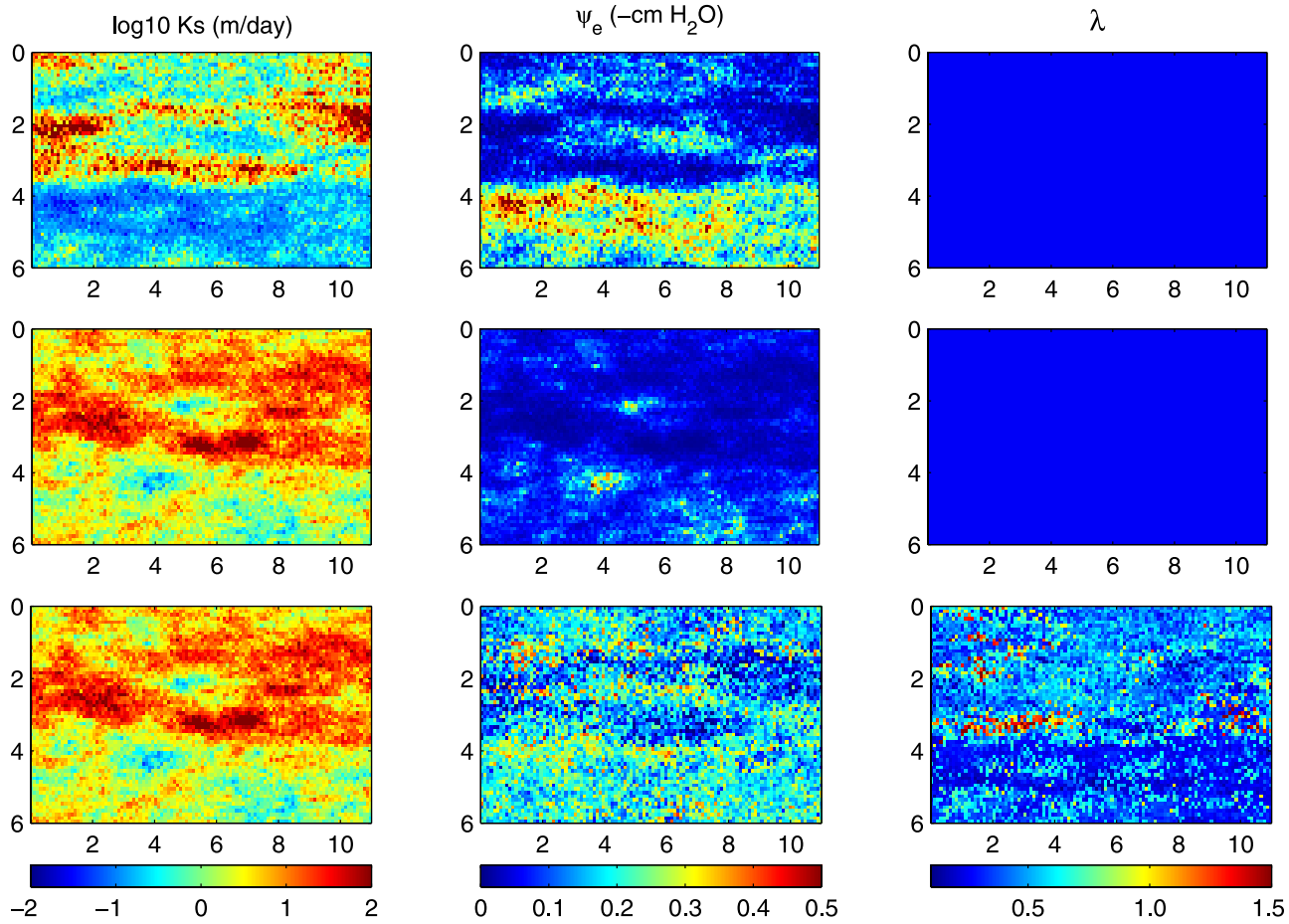

Figure 9. Maps of the spatial distribution of K_s, ψ_e, and λ obtained for one realization with (top) Miller and Miller scaling, (middle) Leverett scaling, and (bottom) the multistep approach.

following the sampled data whereas classes 2 and 4 are scattered throughout the domain, partly because the sampled data are scattered and partly due to the higher relative nugget effect values associated with these classes.

[27] Because the uncertainty in the spatial distribution of K_s must also be incorporated, the soil water retention curve realizations were coupled with one hundred conditional realizations of K_s, assuming independence between K_s and the parameters λ and ψ_e. The assumption of independence is a total departure from the Miller and Miller and the Leverett scaling theories, in which K_s and ψ_e are completely correlated. Still, it is an assumption often made in the literature [*Russo and Bouton*, 1992; *Harter and Yeh*, 1998; *Russo et al.*, 2001; *Zhang and Lu*, 2002] and one that is corroborated by an analysis of soil data in this study, presented in the form of scatterplots shown in Figure 8, and elsewhere [*Hills et al.*, 1992]. Because the distributions of K_s values in the five classes were very similar, the same mean and variance (Table 3) were used in all five classes. The multistep approach could, however, incorporate class-specific statistics of K_s data in the same way values of λ were treated. However, K_s varies only over 4 orders of magnitude in this data set, since the site is composed of basically sandy soils. Had one been dealing with a variability in K_s over more orders of magnitude, for example, with mixed populations of sands and clays, this assumption may not be valid, and individual simulations of K_s within each soil class should be adopted, as *Dillard et al.* [1997] proposed.

3.3. Numerical Flow and Transport Model

[28] The realizations of soil hydraulic properties generated as described in Section 3.2 with the three models of spatial heterogeneity were input into a water flow and solute transport numerical model, a modified version of HYDRUS-2D [*Simunek et al.*, 1999]. The code was modified so that soil physical properties such as K_s and the parameters describing the $\theta(\psi)$ curve could be assigned to elements instead of to nodes in the finite element mesh [*Oliveira*, 2004] and also to compute metrics for the subsequent analysis, such as time of first arrival at different horizontal planes. On the basis of the work by *Rockhold et al.* [1996], D^* was set equal to 1×10^{-4} m^2/d, and D_L and D_T were set equal to 3×10^{-2} m and 3×10^{-3} m, respectively.

[29] In this study, the center of the trench was considered. A subdomain 11 m wide and 6 m deep (the horizontal center of the subdomain coincides with the horizontal center of the trench) was discretized by a regular finite element mesh of triangles with horizontal and vertical sides of 10 cm. Trial runs with a finer grid of 10 cm (horizontal) $\times$ 2.5 cm (vertical) produced results with similar moments and concentration profiles, but increased the total computational time from 25 minutes to 358 minutes, almost a 14 fold increase. Accordingly, the coarser grid was utilized in this

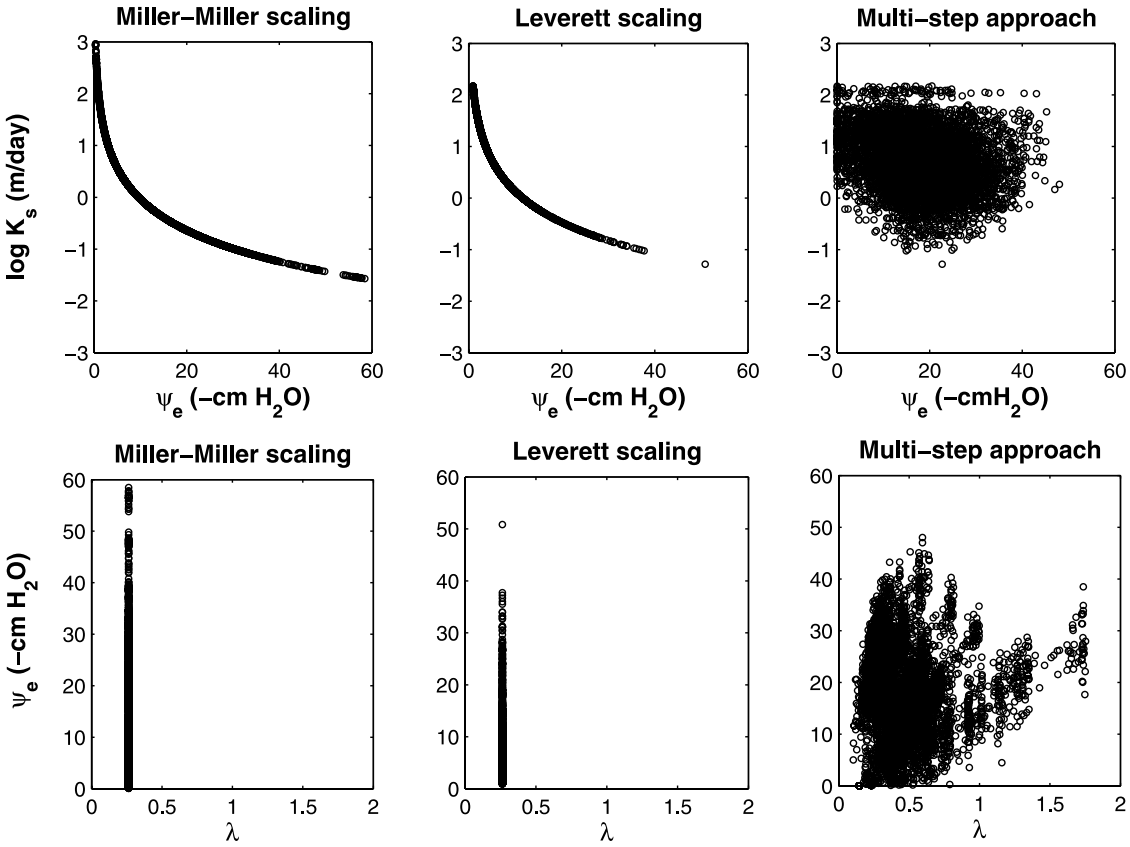

Figure 10. Scatterplots of (top) K_s (m/d) versus ψ_e (cm H_2O) and (bottom) ψ_e (cm H_2O) versus λ (dimensionless) for the realizations shown in Figure 9.

study. The boundary conditions for water flow consisted of no flow boundaries at the sides of the domain, a unit gradient boundary condition at the bottom boundary, and a variable volumetric flux at the top boundary:

$$I(t) = \begin{cases} 1.82\,\text{cm/d} & \text{for } t \le 70\,\text{days} \\ 23\,\text{cm/year} & \text{for } t > 70\,\text{days} \end{cases} \quad (23)$$

for 4.9 m $\le x \le$ 6.1 m, and

$$I(t) = 23\ \text{cm/year for } t > 0\ \text{days} \quad (24)$$

for 0 m $\le x <$ 4.9 m and for 6.1 m $< x \le$ 11 m. The constant rate of 23 cm/year corresponds to the precipitation reported for the site [*Wierenga et al.*, 1989] and the pulse of 1.82 cm/d corresponds to the infiltration rate applied in experiment 2 [*Wierenga et al.*, 1990]. For the solute transport, a no-flow boundary condition was set everywhere except at the bottom

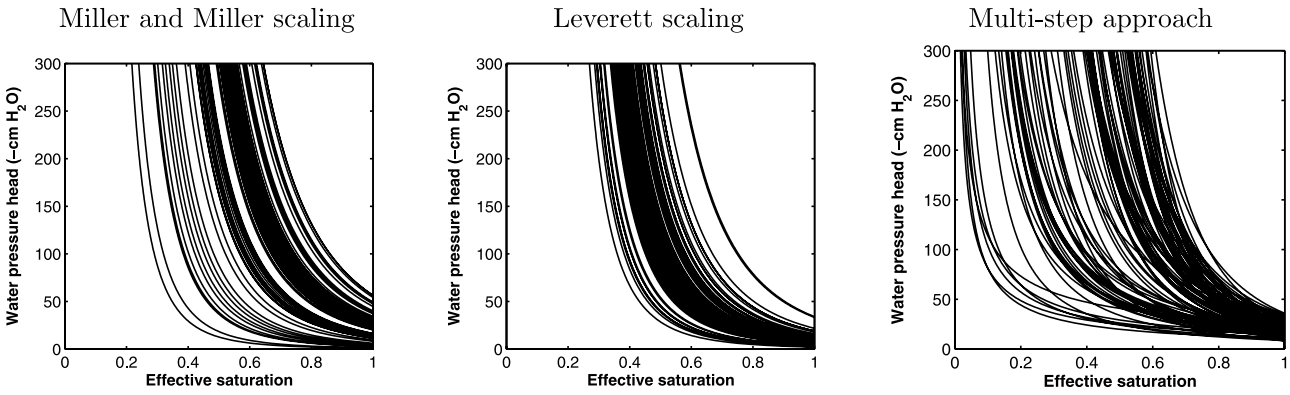

Figure 11. Water retention curves for 100 randomly selected locations in the domains shown in Figure 9 (the same set of locations were used for all three).

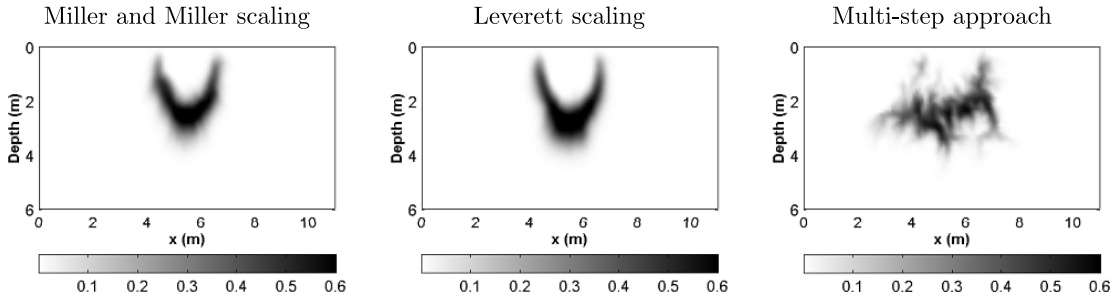

Figure 12. Normalized concentration plume profiles at day 150 obtained using the maps of soil properties displayed in Figure 9.

boundary where a free flow condition was set, and at the top boundary for 4.9 m $\leq x \leq$ 6.1 m, where a variable solute mass flux was set of

$$Q(t) = I(t)C_0;\ C_0 = 1 \text{ for } 29 \leq t \leq 44 \text{ days} \tag{25}$$

where C_0 is a normalized concentration. To obtain an initial field of water pressure heads that reflected the heterogeneity at the site, the domain was subjected to a uniform infiltration rate of 23 cm/year at the top boundary for 1000 days with unit gradient boundary at the bottom and no-flow boundary conditions on the sides. The period of 1000 days was a sufficient time for the pressure heads in the system to reach a quasi-steady state. Cumulative water and solute mass balance errors were, on average, on the order of 0.001% and 1%, respectively.

[30] The effect of the various spatial variability models on the transport of a conservative solute was assessed through the analysis of metrics derived from the simulations' results. The spatial moments of the solute plume at a time, t, are given by [*Russo*, 1991]

$$M_{ij}(t) = \int_{-\infty}^{+\infty} \int_{-\infty}^{+\infty} \theta(x,z,t)C(x,z,t)x^i z^j dxdz \tag{26}$$

The zeroth moment, M_{00}, is the amount of mass within the domain. The first normalized moments represent the position of the centroid of the plumes in the x and z directions and were computed, respectively, as

$$x_c = \frac{M_{10}}{M_{00}} \text{ and } z_c = \frac{M_{01}}{M_{00}} \tag{27}$$

and the second normalized moments, which represent the spread of the plume about the center of mass in the x and z directions, were computed as

$$\sigma_{xx}^2 = \frac{M_{20}}{M_{00}} - x_c^2 \text{ and } \sigma_{zz}^2 = \frac{M_{02}}{M_{00}} - z_c^2 \tag{28}$$

The mean value of these metrics were calculated, after 150 days of simulation, for various numbers of realizations up to 100, when they were observed to have stabilized. Thus 100 realizations of the distribution of soil hydraulic properties were generated using the Miller and Miller, the Leverett, and the multistep approaches, and were then input into the modified version of HYDRUS-2D.

[31] Times of first arrival for a normalized concentration threshold of 10^{-4} at a depth of 3 m were also recorded for each simulation. The statistics for the ensemble of time of first arrivals for each scenario can be used, for example, to assess how long it would take for the plume to reach a point of compliance, such as the water table or a drinking water well, and the uncertainty associated with this time.

4. Results and Discussion

[32] Figure 9 shows the maps of the first of one hundred realizations of the spatial distribution of K_s, ψ_e and λ generated using the three approaches described in Section 3.2. The ψ_e field generated using Miller and Miller scaling (top row) has a balanced proportion of low and high values, with high values occupying predominantly the bottom of the domain. Consequently, the K_s field generated by scaling also has a similar balance of low and high values, with lower values in the bottom part of the domain. The K_s field resulting from the SGS algorithm (middle row) displays a

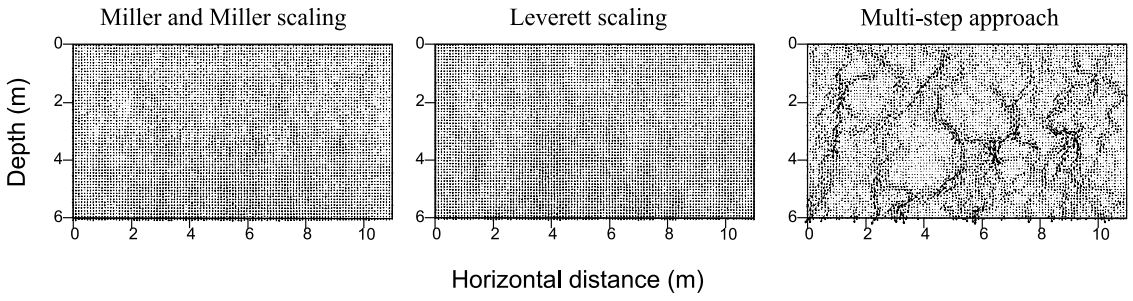

Figure 13. Velocity fields at day 150 corresponding to simulations using the soil properties displayed in Figure 9.

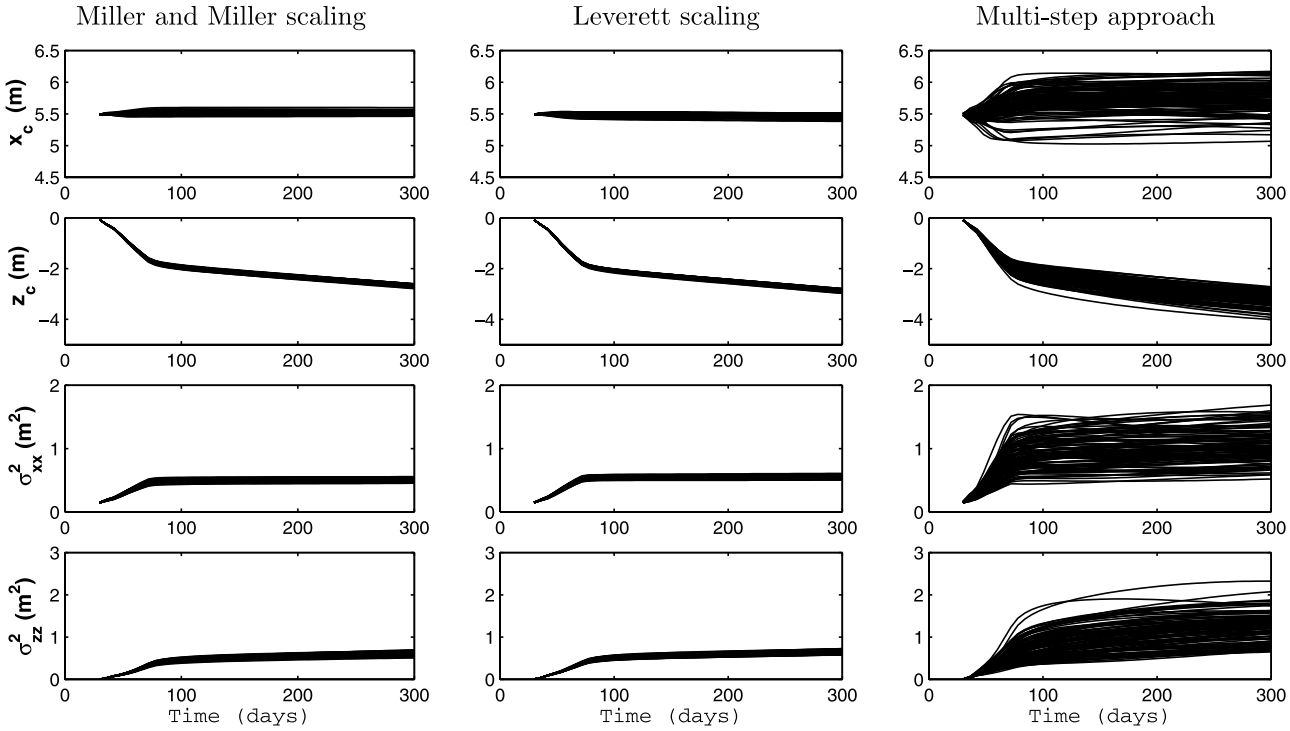

Figure 14. Temporal evolution of the spatial moments of the solute plume using the three approaches for soil transport property characterization. Here x_c and z_c are defined by equation (27), and σ^2_{xx} and σ^2_{zz} are defined by equation (28).

larger proportion of high values than the K_s field generated by the Miller and Miller scaling but that reflects the real distribution of K_s in the field. For both scaling approaches, the λ fields correspond to a single uniform value throughout. The ψ_e and λ fields obtained with the multistep approach (bottom row) are significantly different from those created with the scaling techniques: values of λ and ψ_e vary over their respective expected ranges, and, most importantly, the prior categorical simulation generated clear patterns of continuity and contrasting values, especially for λ. Low values of λ corresponding to class 5 predominate in the bottom of the domain, juxtaposed by higher values corresponding to class 1. Conversely, high values of ψ_e, typical of class 5, dominate the bottom region, whereas lower values, typical of class 1, are clustered in the middle section of the trench. The same kind of pattern for ψ_e is seen in the scaling approaches; however, the λ pattern is unique to the multistep approach.

[33] The differences in soil hydraulic properties that the three approaches generate can be readily grasped by examining Figures 10 and 11. Figure 10 shows a complete correlation between the K_s and ψ_e fields generated with the Miller and Miller and also with the Leverett scaling approaches, while the value of λ is constant regardless of the value of $|\psi_e|$. This leads to water retention curves (Figures 11, left, and 11, middle) that lack the behavior observed from field data (Figure 1a). With the multistep approach, on the other hand, K_s and ψ_e are not correlated, as in the original data set. Furthermore, the points on the ψ_e versus λ scatterplot are clustered following the five classes depicted in Figure 5b, with their correlation as well as their variances being reproduced. These distinct relationships lead to water retention curves that have different shapes (Figure 11, right), with multiple crossings, mimicking the original set of curves measured in the field (Figure 1a).

[34] These differences in the approaches to describe the spatial variability of soil hydraulic properties are reflected in the solute transport simulations. Figures 12 and 13 show solute plumes and velocity profiles, respectively, obtained after 150 days of solute transport simulation using the fields of soil hydraulic properties depicted in Figure 9. The Miller and Miller approach produced plume profiles that were, in general, a little wider and shallower than those obtained with the Leverett scaling, but both methods generated very smooth plume shapes, as if they were simulated in homogeneous domains, with very little variation among realizations. Their velocity profiles were also very smooth with virtually no signs of preferential flow. It is interesting to note that the plume shapes resulting from the simulation of scaled soil hydraulic properties are very similar to those reported by *Rockhold et al.* [1996], despite the fact that

Table 7. Mean and Standard Deviation of the First and Second Spatial Moments of the Contaminant Plume After 150 days of Simulation

	Miller and Miller		Leverett		Multistep	
Metric	Mean	SD	Mean	SD	Mean	SD
x_{c_2} m	5.52	0.025	5.47	0.023	5.72	0.218
σ^2_{xx}, m^2	0.49	0.023	0.55	0.020	0.98	0.258
z_{c_2} m	−2.15	0.039	−2.30	0.035	−2.54	0.247
σ^2_{zz}, m^2	0.51	0.033	0.56	0.030	0.96	0.336

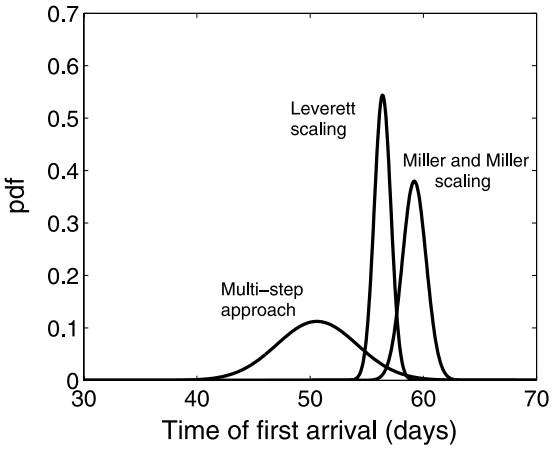

Figure 15. Probability density functions of times of first arrival for 100 realizations of a normalized concentration of 10^{-4} at a horizontal plane located at a depth of 3 m. These distributions were derived from the means and standard deviations shown in Table 8.

another part of the trench was used in that study as well as a slightly different set of initial conditions. On the other hand, the multistep approach produced complex plume shapes, as exemplified in Figure 12, a direct consequence of several preferential pathways that were created in the domains (Figure 13). These preferential flow paths changed from one realization to another, leading to plumes of various shapes.

[35] The reason for this divergent behavior of simulated plumes using the multistep approach lies in the fact that the shape of the unsaturated hydraulic conductivity curve, $K(\psi)$, depends on λ (equation (6)). The value of λ used in the scaling approaches was 0.2631. In the multistep approach, however, the λ values were higher (the median value was 0.420 (Table 4)), a direct consequence of the approach used to fit to the Brooks-Corey function (section 3.2.3). These high values of λ cause a rapid reduction of unsaturated hydraulic conductivity as $|\psi|$ increases. Therefore adjacent cells having high values of λ will act as barriers to water flow, since they lose their capacity to conduct water very quickly, while adjacent cells having low values of λ will give rise to preferential pathways since they maintain relatively high unsaturated hydraulic conductivities at high $|\psi|$.

[36] The spatial distribution of the soil water retention curve parameters dominates the determination of the flow pathways while the saturated hydraulic conductivity plays a secondary role. This is demonstrated here by observing that the Leverett scaling and the multistep approaches share the same K_s fields; therefore the differences in their predicted solute plumes may be attributable to the variability of λ and ψ_e which control the soil water retention curve and the unsaturated hydraulic conductivity function. This is further demonstrated by *Oliveira* [2004], who generated and ran two sets of simulations: one where the K_s field was kept constant while ψ_e and λ changed and another where K_s field changed while ψ_e and λ were kept constant. There, also, a clear predominance of the water retention curve parameters over the saturated hydraulic conductivity in determining the preferential pathways was observed.

[37] Figure 14 shows the temporal evolution of each of the spatial moments for the three approaches examined here. Both scaling methods provided a very similar evolution of moments despite the large differences observed for the K_s and ψ_e fields (Figure 9). The first and second moments of the 100 simulations produced using the scaling methods had very small standard deviations (Table 7). The larger spread in values of x_c and z_c for the multistep approach reflects the fact that the plumes assumed various shapes, sometimes shallow and wide, sometimes deep and narrow. The spaces of uncertainty of the first moments, x_c and z_c, encompass the ones obtained with the scaling techniques (Figure 14 and Table 7), indicating that the method provides conservative estimates for these metrics, as its results cover a broader spectrum of possibilities than those obtained with scaling techniques. The ensemble metrics therefore show a very different picture from those resulting from use of the scaling techniques, with higher values for the mean and for the standard deviation of σ^2_{xx} and σ^2_{zz}.

[38] First arrival times for a normalized concentration of 10^{-4} at a plane located at a depth of 3 m were recorded for each simulation. Basic statistics of these sets of values are shown in Table 8. Normal probability density functions for each one, derived from their respective means and standard deviations, are shown in Figure 15. The distribution of times of first arrival predicted by each approach did not overlap much, with the spread around the mean being much smaller for the scaling approaches than for the multistep approach. The predicted times are shorter using Leverett scaling than using Miller and Miller, with mean values of 56.4 and 59.2 days, respectively, which may be explained by the higher values of K_s present in the domains obtained with Leverett scaling. The multistep simulations predicted a mean time of first arrival of 50.6 days and the upper tail of its time pdf overlaps the pdf of Leverett scaling times. In addition, the mean time predicted with the Miller and Miller scaling exceeds the maximum time obtained with the multistep approach (Table 8). Thus the multistep approach would lead to a more conservative assessment of the uncertainty about the time that a solute would take to move through the unsaturated zone.

5. Conclusion

[39] The results presented here show that the scaling approaches, despite having different K_s and ψ_e fields, led to concentration plumes with very similar shapes, similar spatial moments and similarly narrow spaces of uncertainty. Although the primary data fields used in these methods (either the soil water retention curves or the saturated hydraulic conductivity) vary among realizations, the result-

Table 8. Statistics for Times of First Arrival of a Normalized Concentration Threshold of 10^{-4} at a Depth of 3 m[a]

Approach	Minimum	Maximum	Mean	Standard Deviation
Miller and Miller scaling	56.25	61.39	59.19	1.045
Leverett scaling	54.75	58.40	56.45	0.734
Multistep approach	42.41	58.35	50.60	3.546

[a]Values are in days.

ing concentration plumes were all alike and their shapes resemble those obtained using homogeneous fields, although the heterogeneity of the Las Cruces Trench is well established [*Hills et al.*, 1992]. The assumption of a strict correlation between K_s and ψ_e fields, along with a uniform λ field, seems to be unrealistic and produces results that potentially obscure the real properties of the site. The water contents coalesced very well in the Miller and Miller approach [*Rockhold et al.*, 1996; *Oliveira*, 2004]; yet, using the same scaling factors to predict K_s couples the properties in a way that is not supported by field data. Similarly, starting with saturated hydraulic conductivity information and applying Leverett scaling to predict water retention curves, establishes a strict correlation that may not exist. The results here therefore echo the conclusions of *Jury et al.* [1987a], that both the soil water retention parameters and the saturated hydraulic conductivity need to be analyzed separately. Another drawback of the scaling methods is that if only measurements of one property are available, choosing the reference parameters for the second set of properties (either ψ_e^* and λ^* in the Leverett scaling or K_s^* in the Miller and Miller scaling) is either subjective or requires some additional measurements. Depending on the set of reference parameters chosen, the scaling procedure can potentially result in unrealistic predictions of soil properties in the domain. For example, a quick calculation shows that for the lowest permeability value in *Dillard et al.* [1997], $10^{-18.75}$ m^2, corresponds to a value of 6.5×10^{-4} m^{-1} for the van Genuchten shape parameter α [*van Genuchten*, 1980], producing a soil with an air-entry pressure head of approximately $-60{,}000$ cm H_2O.

[40] Assuming the existence of measurements of both soil water retention curves and saturated hydraulic conductivities, the multistep approach showed the potential to generate preferential flow paths, thus capturing the impacts of the heterogeneity of a soil's hydraulic properties on the flow of water and solute transport in the unsaturated zone. It may be argued that the differences seen in the multistep technique result solely from the use of additional information. Even so, it shows the importance of measuring and analyzing K_s and $\theta(\psi)$ independently, rather than relying on one property to generate information about the other. Because the K_s distributions looked similar across the soil classes (Figure 8), the same mean and variance were used throughout (Table 3). The multistep approach could, however, incorporate class-specific statistics of K_s data in the same way values of λ were generated. The potential spatial cross correlation between soil classes was not considered nor was the spatial cross correlation between λ and ψ_e within classes. These aspects deserve further investigation, particularly for sites where the hydraulic conductivity varies over several orders of magnitude, such as the Bemidji site, where K_s varies over nine orders of magnitude [*Dillard et al.*, 1997].

[41] **Acknowledgments.** We would like to thank Jirka Simunek for providing the source code of HYDRUS-2D and for helpful comments concerning the modification of the code. Thanks are also owed to Peter Wierenga and Richard Hills for providing the Las Cruces Trench Site data. Mark Rockhold is acknowledged for helpful discussions regarding the Las Cruces data. We also would like to thank the two anonymous reviewers for their comments and suggestions. Funding for this work was provided by a fellowship from CNPq (Conselho Nacional de Desenvolvimento Científico e Tecnológico–Brazil) to the first author under grant 200765/98-1 and from the Department of Civil and Environmental Engineering at the University of Michigan.

References

Ahuja, L. R., J. Naney, and D. R. Nielsen (1984), Scaling soil water properties and infiltration modeling, *Soil Sci. Soc. Am. J.*, *48*, 970–973.

Alabert, F. G., G. J. Massonnat, and E. Aquitaine (1990), Heterogeneity in a complex turbiditic reservoir: Stochastic modeling of facies and petrophysical variability, *SPE Pap. 20604*, Soc. of Pet. Eng., Richardson, Tex.

Bear, J. (1972), *Dynamics of Fluids in Porous Media*, 764 pp., Dover, Mineola, N. Y.

Brooks, R. H., and A. T. Corey (1964), Hydraulic properties of porous media, *Hydrol. Pap. 3*, Colo. State Univ., Fort Collins.

Brooks, R. H., and A. T. Corey (1966), Properties of porous media affecting fluid flow, *Proc. Am. Soc. Civ. Eng.*, *92*, 61–88.

Burdine, N. T. (1953), Relative permeability calculations from pore size distribution data, *Trans. Am. Inst. Min. Metall. Pet. Eng.*, *198*, 71–78.

Chen, G., and S. P. Neuman (1996), Wetting front instability in randomly stratified soils, *Phys. Fluids*, *8*(2), 353–369.

Clausnitzer, V., J. W. Hopmans, and D. R. Nielsen (1992), Simultaneous scaling of soil water retention and hydraulic conductivity curves, *Water Resour. Res.*, *28*, 19–31.

Corey, A. T., and R. H. Brooks (1999), The Brooks-Corey relationships, in *Proceedings of the International Workshop on Characterization and Measurement of the Hydraulic Properties of Unsaturated Porous Media*, edited by M. T. van Genuchten, F. J. Leij, and L. Wu, pp. 13–18, Univ. of Calif., Riverside.

Damsleth, E., C. B. Tjølsen, H. Omre, and H. H. Haldorsen (1992), A two-stage stochastic model applied to a North Sea reservoir, *J. Pet. Technol.*, *44*(4), 402–408.

Desbarats, A. J. (1995), Upscaling capillary pressure–saturation curves in heterogeneous porous media, *Water Resour. Res.*, *31*(2), 282–288.

Deurer, M., W. H. M. Duijnisveld, and J. Böttcher (2000), Spatial analysis of water characteristic functions in a sandy podzol under pine forest, *Water Resour. Res.*, *36*(10), 2925–2935.

Deutsch, C. V., and A. G. Journel (1998), *GSLIB: Geostatistical Software Library and User's Guide*, 2nd ed., 340 pp., Oxford Univ. Press, New York.

Dillard, L., H. I. Essaid, and W. N. Herkelrath (1997), Multiphase flow modeling of a crude-oil spill site with a bimodal permeability distribution, *Water Resour. Res.*, *33*(7), 1617–1632.

Draper, N. R. (1981), *Applied Regression Analysis*, 2nd ed., 709 pp., John Wiley, Hoboken, N. J.

Essaid, H. I., W. N. Herkelrath, and K. Hess (1993), Simulation of fluid distributions observed at a crude oil spill site incorporating hysteresis, oil entrapment, and spatial variability of hydraulic properties, *Water Resour. Res.*, *29*, 1753–1770.

Gerhard, J. I., and B. H. Kueper (2003), Influence of constitutive model parameters on the predicted migration of DNAPL in heterogenous porous media, *Water Resour. Res.*, *39*(10), 1279, doi:10.1029/2002WR001570.

Goovaerts, P. (1997), *Geostatistics for Natural Resources Evaluation*, 483 pp., Oxford Univ. Press, New York.

Harter, T., and T. C. J. Yeh (1996), Conditional stochastic analysis of solute transport in heterogeneous, variably saturated soils, *Water Resour. Res.*, *32*, 1597–1609.

Harter, T., and T. J. Yeh (1998), Flow in unsaturated random porous media, nonlinear numerical analysis and comparison to analytical stochastic models, *Adv. Water Resour.*, *22*(3), 257–272.

Hills, R. G., and P. Wierenga (1991), Model validation at the Las Cruces Trench Site, *Tech. Rep. NUREG/CR-5716*, U. S. Nucl. Regul. Comm., Washington, D. C.

Hills, R. G., P. J. Wierenga, D. B. Hudson, and M. R. Kirkland (1991), The second Las Cruces Trench Site experiment: Experimental results and two-dimensional flow predictions, *Water Resour. Res.*, *27*(10), 2702–2718.

Hills, R. G., D. B. Hudson, and P. J. Wierenga (1992), Spatial variability at the Las Cruces Trench Site, in *Proceedings of the International Workshop on Indirect Methods for Estimating the Hydraulic Properties of Unsaturated Soils, Riverside, California, October 11–23, 1989*, edited by M. T. v. Genuchten, F. J. Leij, and L. J. Lund, pp. 529–538.

Hills, R. G., P. Wierenga, S. Luis, D. McLaughlin, M. Rockhold, J. Xiang, B. Scanlon, and G. Wittmeyer (1993), INTRAVAL - Phase II model testing at the Las Cruces Trench Site, *Tech. rep.*, U. S. Nuclear Regulatory Commission – NUREG/CR-6063, Washington, D. C.

Hopmans, J. W. (1992), Scaling applications in soil characterization, in *International Workshop on Indirect Methods for Estimating the Hydrau-*

lic Properties of Unsaturated Soils, Riverside, California, October 11–13 (1989), edited by M. T. van Genuchten, F. J. Leij, and L. J. Lund, pp. 539–551, Univ. of Calif., Riverside.

Hopmans, J. W., H. Schukking, and P. J. J. Torfs (1988), Two-dimensional steady state unsaturated water flow in heterogeneous soils with autocorrelated soil hydraulic properties, *Water Resour. Res.*, *24*, 2005–2017.

Jacobson, E. A. (1990), Investigation of the spatial correlation of saturated hydraulic conductivities from a vertical wall of a trench, in paper presented at Canadian/American Conference on Hydrogeology: Parameter Identification and Estimation for Aquifer and Reservoir Characterization, Altantic Res. Counc., Calgary, Alberta, Canada, 18–20 Sept.

Journel, A. G. (1983), Nonparametric estimation of spatial distributions, *Math. Geol.*, *15*(3), 445–468.

Jury, W. A., D. Russo, G. Sposito, and H. Elabd (1987a), The spatial variability of water and solute transport properties in unsaturated soil. I. Analysis of property variation and spatial structure with statistical models, *Hilgardia*, *55*(4), 1–32.

Jury, W. A., D. Russo, G. Sposito, and H. Elabd (1987b), The spatial variability of water and solute transport properties in unsaturated soil. II. Scaling models of water transport, *Hilgardia*, *55*(4), 33–56.

Lemke, L. D., L. M. Abriola, and P. Goovaerts (2004), Dense nonaqueous phase liquid DNAPL source zone characterization: Infuence of hydraulic property correlation on predictions of DNAPL infiltration and entrapment, *Water Resour. Res.*, *40*, W01511, doi:10.1029/2003WR001980.

Leverett, M. C. (1941), Capillary behavior in porous solids, *Trans. Am. Inst. Min. Metall. Pet. Eng.*, *142*, 152–169.

Miller, E. E., and R. D. Miller (1955a), Theory of capillary flow: I. Pratical implications, *Soil Sci. Soc. Am. Proc.*, *19*(5), 267–271.

Miller, R., and E. Miller (1955b), Theory of capillary flow: II. Experimental information, *Soil Sci. Soc. Am. Proc.*, *19*(5), 271–275.

Miller, E. E., and R. D. Miller (1956), Physical theory for capillary flow phenomena, *J. Appl. Phys.*, *27*(4), 324–332.

Oliveira, L. I. (2004), An assessment of the benefit of additional physical site characterization for modeling the field-scale transport of solutes in a heterogeneous unsaturated soil, Ph.D. thesis, Dep. of Civ. and Environ. Eng., Univ. of Mich, Ann Arbor.

Peck, A. J., R. J. Luxmoore, and J. L. Stolzy (1977), Effects of spatial variability of soil hydraulic properties in water budget modeling, *Water Resour. Res.*, *13*, 348–354.

Philip, J. R. (1975), Stability analysis of infiltration, *Soil Sci. Soc. Am. Proc.*, *39*, 1042–1049.

Rockhold, M. L., R. E. Rossi, and R. G. Hills (1996), Application of similar media scaling and conditional simulation for modeling water flow and tritium transport at the Las Cruces Trench Site, *Water Resour. Res.*, *32*(3), 595–609.

Russo, D. (1991), Stochastic analysis of simulated vadose zone solute transport in a vertical cross section of heterogeneous soil during nonsteady water flow, *Water Resour. Res.*, *27*(3), 267–283.

Russo, D., and M. Bouton (1992), Statistical analysis of spatial variability in unsaturated flow parameters, *Water Resour. Res.*, *28*(7), 1911–1925.

Russo, D., and E. Bresler (1980), Scaling soil hydraulic properties of a heterogeneous field, *Soil Sci. Soc. Am. J.*, *44*, 681–684.

Russo, D., J. Zaidel, and A. Laufer (1998), Numerical analysis of flow and transport in a three-dimensional partially saturated heterogeneous soil, *Water Resour. Res.*, *34*(6), 1451–1468.

Russo, D., J. Zaidel, and A. Laufer (2001), Numerical analysis of flow and transport in a combined heterogeneous vadose zone-groundwater system, *Adv. Water Resour.*, *24*, 49–62.

Shouse, P. J., W. B. Russel, D. S. Burden, H. M. Selim, J. B. Sisson, and M. T. van Genuchten (1995), Spatial variability of soil water retention functions in a silt loam soil, *Soil Sci.*, *159*(1), 1–12.

Simunek, J., M. Sejna, and M. T. van Genuchten (1999), The HYDRUS-2D software package for simulating the two-dimensional movement of water, heat and multiple solutes in variably-saturated media, version 2.0, report, 253 pp., Colo. Sch. of Mines, Golden.

Tartakovsky, A. M., S. P. Neuman, and R. J. Lenhard (2003), Immiscible front evolution in randomly heterogeneous porous media, *Phys. Fluids*, *15*(11), 3331–3341.

Tseng, P.-H., and W. A. Jury (1993), Simulation of field measurement of hydraulic conductivity in unsaturated heterogeneous soil, *Water Resour. Res.*, *29*(7), 2087–2099.

van Genuchten, M. T. (1980), A closed-form equation for predicting the hydraulic conductivity of unsaturated soils, *Soil Sci. Soc. Am. Proc.*, *44*, 892–898.

Vogel, T., M. Cislerova, and J. W. Hopmans (1991), Porous media with linearly variable hydraulic parameters, *Water Resour. Res.*, *27*(10), 2735–2741.

Warrick, A. W., G. J. Mullen, and D. R. Nielsen (1977), Scaling field-measured soil hydraulic properties using a similar media concept, *Water Resour. Res.*, *13*, 355–362.

Wierenga, P. J., A. Toorman, D. B. Hudson, J. Vinson, M. Nash, and R. G. Hills (1989), Soil physical properties at the Las Cruces Trench Site, *Tech. Rep. NUREG/CR-5441*, U.S. Nucl. Regul. Comm., Washington, D. C.

Wierenga, P. J., D. B. Hudson, R. G. Hills, I. Porro, M. R. Kirkland, and J. Vinson (1990), Flow and transport at the Las Cruces Trench Site—Experiments 1 and 2, *Tech. Rep. NUREG/CR-5607*, U.S. Nucl. Regul. Comm., Washington, D. C.

Wierenga, P. J., R. G. Hills, and D. B. Hudson (1991), The Las Cruces Trench Site: Characterization, experimental results, and one-dimensional flow predictions, *Water Resour. Res.*, *27*, 2695–2705.

Zhang, D., and Z. Lu (2002), Stochastic analysis of flow in a heterogeneous unsaturated-saturated system, *Water Resour. Res.*, *38*(2), 1018, doi:10.1029/2001WR000515.

L. M. Abriola, Department of Civil and Environmental Engineering, 105 Anderson Hall, Tufts University, Medford, MA 02155, USA.

A. H. Demond and L. I. Oliveira, Department of Civil and Environmental Engineering, University of Michigan, Room 120, 1351 Beal Avenue, Ann Arbor, MI 48109-2125, USA. (averyd@umich.edu)

P. Goovaerts, BioMedware Inc., 516 North State Street, Ann Arbor, MI 48104, USA.